JOURNAL OF PROPULSION AND POWER
Vol. 25, No. 2, March–April 2009

Film Cooling of Accelerated Flow in a Subscale Combustion Chamber

R. Arnold,* D. Suslov,† and O. J. Haidn‡
DLR, German Aerospace Center, 74239 Hardthausen, Germany

DOI: 10.2514/1.39308

Experimental investigations have been carried out to examine film cooling effectiveness of an accelerated hot gas in a subscale rocket combustion chamber. In support of future first-stage high-performance rocket combustion chambers, a Vulcain-2-like test case has been examined with combustion pressure levels up to 12 MPa. The effectiveness of an almost tangentially injected film of hydrogen with an initial temperature of ≈280 K has been determined. Axial distributions of temperature were measured inside the copper liner as well as on the chamber surface in the convergent and divergent parts of the nozzle segment. An existing film cooling model has been modified for application in a combined convective and film-cooled combustion chamber with an accelerated hot gas. The new model predicts film cooling effectiveness at different combustion-chamber pressures and film blowing rates at sub-, trans-, and supersonic conditions.

Nomenclature

a_1, a_2	=	parameters
b	=	injection slot width, mm
c_p	=	specific heat capacity for constant pressure, J/kgK
D	=	chamber diameter, mm
d	=	distance from the hot-gas side, mm
f	=	function, correction factor
I_s	=	specific impulse, s
M	=	film blowing rate
Ma	=	Mach number
$\dot{m}$	=	mass flow rate, kg/s
Pr	=	Prandtl number
p	=	pressure, MPa
$\dot{q}$	=	heat flux, W/m^2
Re	=	Reynolds number
ROF	=	mixture ratio of oxidizer/fuel
s	=	injection slot height, mm
T	=	temperature, K
t	=	time, s
u	=	velocity, m/s
x	=	distance downstream from the point of film injection, mm
β	=	injection parameter
γ	=	angle of film coolant injection, deg
$\Delta\Theta^*$	=	difference of film cooling effectiveness
ζ	=	parameter
η	=	adiabatic film cooling effectiveness for uniform mainstream velocity
η^*	=	adiabatic film cooling effectiveness for accelerated flow
Θ	=	film cooling effectiveness for uniform mainstream velocity
Θ^*	=	film cooling effectiveness for accelerated flow
μ	=	dynamic viscosity, kg/ms
ρ	=	density, kg/m^3

Subscripts

ad	=	adiabatic
cc	=	combustion chamber, hot gas, mainstream
f	=	film cooling
max	=	maximum
min	=	minimum
t	=	nozzle throat
tot	=	total
W	=	wall
0	=	without film cooling
2	=	film at point of injection

I. Introduction

SURFACES in a rocket engine combustion chamber are exposed to extremely high thermal and structural loads during the hot run and transient operation. Assuming constant engine dimensions, enhanced engine performance for next-generation first-stage rocket engines can only be realized with an increase of propellant mixing ratio ROF and chamber pressure p_{cc}, although both mean an additional increase in structural as well as in thermal loads of the combustion-chamber walls. A higher combustion-chamber pressure results in an almost linear increase of the heat flux level $\dot{q}$ from the hot gas to the liner materials [1]:

$$\dot{q} \propto p_{cc}^{0.8} \tag{1}$$

High temperature differences between the hot combustion gases and the chamber walls in conjunction with combustion-chamber pressures of more than 18 MPa [for example, in the space shuttle main engine (SSME) ($p_{cc} = 19$ MPa [2]) or in the RD-170 ($p_{cc} = 24.8$ MPa [3])] result in extremely high heat flux levels and temperature gradients through the combustion chamber. A regenerative cooling system alone is insufficient in high-performance rocket engines because of pressure drop in the cooling channels as well as manufacturing and structural limits, and regenerative cooling has to be augmented with an additional film cooling system. Thus, modern first-stage rocket engines use film cooling not only in the immediate vicinity of the injector head (e.g., Vulcain 2, SSME), either with slot injection of gaseous or liquid coolant by a reduction of the mixture ratio ROF in the vicinity of the wall (injector trimming) or by angling (biasing) of the liquid-oxygen posts of the outer injector elements away from the combustion-chamber walls, but also in the region of the nozzle throat section (e.g., RD-170) [4–6].

Received 25 June 2008; revision received 20 November 2008; accepted for publication 30 November 2008.

*Ph.D. Student, Institute of Space Propulsion, Lampoldshausen; richard.arnold@dlr.de. Member AIAA (Corresponding Author).

†Research Engineer, Institute of Space Propulsion, Lampoldshausen; dmitry.suslov@dlr.de.

‡Head of Technology, Institute of Space Propulsion, Lampoldshausen; oskar.haidn@dlr.de. Associate Fellow AIAA.

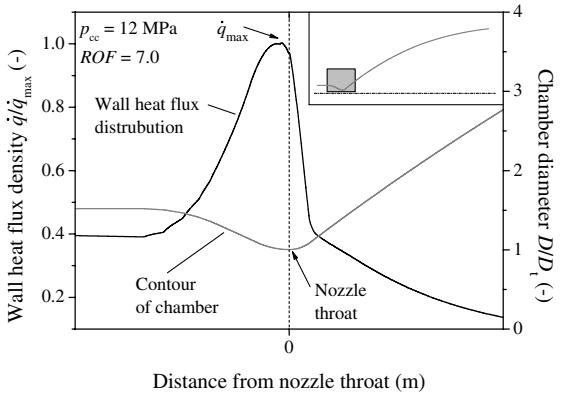

Fig. 1 Calculated wall heat flux distribution in the nozzle throat section.

Future rocket engines with high combustion-chamber pressures will therefore not only use film cooling in the cylindrical part of the combustion chamber, but also in the nozzle throat region, in which maximum heat fluxes occur and effective cooling of the structure is essential for reliable operation. A miscalculation of merely 40 K of the predicted wall temperature can result in a halving of the engine durability [7].

Despite substantial progress in numerical simulation during the last years, realistic experimental data at representative enginelike conditions for further verification and development of numerical film cooling design tools still do not exist in the open literature. Although there have been only a few experimental investigations on film cooling in rocket combustion chambers, the influence of an accelerated hot gas at these conditions on film cooling effectiveness has been considered even less in the past [8,9].

Because maximum heat flux occurs in close proximity to the nozzle throat, effective cooling of the throat area is crucial for enhanced engine reliability and lifetime. Figure 1 reveals the significant growth of the wall heat-load distribution in the nozzle throat section for a typical engine with a chamber pressure of $\approx$12 MPa and a propellant mixture ratio of 7.0, calculated with the two-dimensional-kinetics nozzle-performance computer program TDK91/PRO [10]. Very high heat flux gradients in combination with an accelerated hot gas complicate the design of an efficient cooling scheme and underline the need for additional film cooling in the region of accelerated flow in the nozzle throat area.

To provide fundamental knowledge of film cooling of an accelerated hot gas, an almost tangential film has been injected at the beginning of the nozzle segment of a subscale rocket combustion chamber using supercritical hydrogen as a film coolant at various film blowing rates. A correlation between film effectiveness in nonaccelerated flow and accelerated flow has been developed to describe film cooling effectiveness at the nozzle throat region. Experimental results as well as a correlation to predict film cooling effectiveness in combination with accelerated hot gas in the sub-, trans-, and supersonic regions of a subscale rocket combustion chamber are presented in the body of the paper.

II. Film Cooling

In rocket engines, film cooling is a widely used cooling method to protect the combustion-chamber walls from hot combustion gases. Either a liquid or gaseous cooling film is introduced into the combustion chamber through slots or orifices, which protects the chamber walls not only in the vicinity of the injection, but also farther downstream, a distance of some hundred film-coolant-slot heights.

A. Film Cooling Effectiveness

For describing and comparing different film cooling results and models, adiabatic film cooling effectiveness η is a widely used parameter in literature [11–13]. The difference between adiabatic wall temperature T_{ad} and hot-gas temperature T_{cc} is referred to the maximum difference between coolant temperature at the point of injection T_2 and hot-gas temperature:

$$\eta = \frac{T_{ad} - T_{cc}}{T_2 - T_{cc}} \tag{2}$$

However, this definition of film cooling effectiveness is difficult to apply in a rocket engine combustion chamber, due to very high temperatures of the combustion gases of up to almost 3800 K. Adiabatic wall temperatures would exceed safe operating temperatures of all known combustor materials. Hence, for a high-pressure rocket combustion chamber that uses convective and film cooling in combination, it is necessary to establish another temperature ratio Θ to describe film cooling effectiveness. This temperature ratio can be used as a degree of effectiveness for film cooling processes. The local temperature difference due to the application of film cooling will be compared with the maximal achievable temperature difference, where $T_{W,0}$ designates the wall temperature without film cooling and $T_{W,f}$ designates the wall temperature with film cooling:

$$\Theta(x) = \frac{T_{W,0}(x) - T_{W,f}(x)}{T_{W,0}(x) - T_2} \tag{3}$$

Equation (2), as well as Eq. (3), describes the wall-temperature reduction due to film cooling relating to a theoretical maximal temperature reduction. In the presented paper, only nonadiabatic film cooling effectiveness has been measured and will be discussed in the results section.

B. Film Cooling Effectiveness for Uniform Mainstream Velocity

As a first step in developing a model of film cooling of an accelerated flow, film cooling models describing the effectiveness for a uniform mainstream flow will be discussed.

In general, three flow types can be differentiated downstream of a film coolant injection point. In the core zone of the wall-jet region, the wall temperature can be assumed to be the film injection temperature, whereas in the following mixing region, an increase of the wall temperature occurs due to the gradually mixing of hot gas and film coolant. In the boundary-layer region farther downstream, the film effectiveness can be described as a function of the distance from the point of injection at which the mixing of both flows is completed [14,15].

In the past, a number of film-cooling-effectiveness predictions and models, both theoretical and empirical, have been developed. However, most models assume either a complete mixture of the hot gas and film coolant (heat-sink model and boundary-layer model) or no mixing (flow model and wall-jet model). Of course, the heat-sink model will show better results a certain distance downstream of the film injection point, whereas the flow model is more applicable in the vicinity of the coolant injection. Because of the turbulent flow inside the combustion chamber, the assumptions of the heat-sink model will be much more convenient than those of the flow model when describing film cooling in a rocket combustion chamber. On this account, only models assuming complete mixing of the hot gas and film coolant will be considered in the following.

An early heat-sink model has been presented by Tribus and Klein [16] for a turbulent flow on a flat plate:

$$\eta = 5.76 Pr^{2/3} \frac{c_{p,2}}{c_{p,cc}} \zeta^{-0.8} \tag{4}$$

where

$$\zeta = \frac{x}{s} \frac{1}{M} \left(Re_{2,s} \frac{\mu_2}{\mu_{cc}} \right)^{-0.25} \tag{5}$$

and M describes the ratio of mass velocity of the coolant to the hot-gas mass velocity:

$$M = \frac{\rho_2 u_2}{\rho_{cc} u_{cc}} \tag{6}$$

Kutateladze and Leont'ev [17] considered the film cooling effectiveness for small temperature gradients, using a heat balance within the boundary layer, on a flat plate with a tangential injected film coolant:

$$\eta = \left(1 + 0.24 Re_{2,s}^{-0.25} \frac{u_{cc}}{u_2} \frac{x}{s}\right)^{-0.8} \tag{7}$$

Librizzi and Cresci [18] performed a turbulent flow in the convergent and divergent parts of a nozzle with a constant boundary-layer temperature using hot-gas temperatures up to 1400 K:

$$\eta = \left(\frac{1}{1 + 0.329(c_{p,cc}/c_{p,2})\zeta^{0.8}}\right) \tag{8}$$

Goldstein and Haji-Sheikh [13] also used a heat balance within the boundary layer and included temperature variation in the boundary layer as well as the growth of the boundary-layer thickness because of the injection of coolant. For a turbulent incompressible flow, the prediction of film cooling effectiveness is given as

$$\eta = \frac{1.9 Pr^{2/3}}{1 + 0.329(c_{p,cc}/c_{p,2})[(x/s)(1/M)]^{0.8} Re_{2,s}^{-0.2}\beta} \tag{9}$$

The nondimensional parameter β depends on the angle of injection γ between the hot-gas fluid and the film coolant. Any enlargement of the angle of injection results in a reduction of the film cooling effectiveness due to an increased mixing of the film coolant with the hot gas directly at the point of injection:

$$\beta = 1 + 0.15 \times 10^{-3} Re_{2,s} \frac{\mu_2}{\mu_{cc}} \sin\gamma \tag{10}$$

The model has been verified with experimental data from Wieghardt [19], Goldstein et al. [20,21], and Nishiwaki et al. [22] and has shown good agreement for blowing rates M up to ≈ 1.

Despite the large number of film cooling models, none of the aforementioned predictions considers the extreme conditions inside a rocket thrust chamber. Variable fluid properties not only of the hot gas, but also of the coolant (heat capacity, thermal conductivity, and density), large temperature gradients between hot gas and film coolant, high heat flux densities, and combustion-chamber pressures have not been considered. Recombination effects in the vicinity of the chamber wall, acting as an additional heat source, are also ignored in most models. Furthermore, most film cooling models assume the same fluids or fluids with similar characteristics for mainstream flow and film coolant, whereas in a rocket combustion chamber, the fluid properties of hot gas and film coolant are significantly different.

Experimental investigations of film cooling with tangential slot injection in close proximity of the injector head have shown a much faster reduction of film cooling effectiveness in the axial direction than predicted by traditional film cooling models [23,24]. Based on Eq. 9 from Goldstein and Haji-Sheikh [13], a modified empirical prediction has been found for describing the film cooling effectiveness Θ in a regenerative and film-cooled high-pressure rocket combustion chamber for tangential slot injection, considering the influence of comparatively high Reynolds numbers of the injected film coolant [24]:

$$\Theta = \frac{0.83 Pr^{2/3}}{1.11 + 0.329(c_{p,cc}/c_{p,2})[(x/s)(1/M)]^{1.43} Re_{2,s}^{-0.25}} \tag{11}$$

Investigations at the DLR, German Aerospace Center in Lampoldshausen (DLR Lampoldshausen) with combustion-chamber pressures of 11.5, 8, and 5 MPa at various film blowing rates M have shown good agreement with the modified film cooling model, following Eq. (11) [24].

C. Film Cooling Effectiveness with Accelerated Hot Gas

Although there have been some studies of film cooling with accelerating mainstream velocity, there are no existing models describing film cooling effectiveness satisfactorily in the converging and diverging parts of a nozzle segment. Based on a description of film cooling effectiveness for a uniform mainstream velocity, a model for accelerated hot gas has been found by multiplying the constant-velocity effectiveness with a function that characterizes the accelerated flow.

Investigations of film cooling effectiveness with a freestream pressure gradient along a flat plate have been conducted by Seban and Back [25] and Hartnett et al. [26]. Hartnett et al. proposed to multiply the adiabatic film cooling effectiveness predicted for uniform mainstream velocity by a function of the local mainstream velocity to consider acceleration effects [26]:

$$\eta^*\left(\frac{x}{s}\right) = \eta\left(\frac{x}{s}\right) \cdot \left(\frac{u_{cc}}{u_{cc,(x/s)=0}}\right)^{0.2} \tag{12}$$

Most of the film cooling studies dealing with accelerated flow reported relatively small change in film cooling effectiveness compared with results for uniform mainstream velocity (e.g., Hartnett et al. [26], Seban and Back [25], Escudier and Whitelaw [27]). However, Carlson and Talmor [28] measured a large decrease of the film cooling effectiveness with acceleration of the main flow for nontangential injection. None of the models considered acceleration due to a high pressure gradient in combination with a fully turbulent flow and very high temperatures of the main flow with variable fluid properties. The impacts on boundary-layer thickness due to the acceleration of the hot gas and coolant entering the boundary layer as well as potential relaminarization of localized turbulence due to acceleration effects are not described in conventional film cooling models. Furthermore, the influence of acceleration on film cooling effectiveness cannot be described only by numerical simulation. Experimental investigations with engine-like conditions are necessary for the basic understanding of film cooling processes with accelerated hot gas in a rocket combustion chamber.

Analysis of film cooling in combination with an accelerated main flow described in this paper will use a similar approach to that suggested by Hartnett et al. [26]. However, because acceleration conditions inside a rocket combustion chamber are different from freestream acceleration

$$\left(T, p, u, c_p = f\left(\frac{x}{s}\right)\right)$$

a function of the local Mach number will be used instead of the velocity ratio to describe the film cooling effectiveness Θ^* in the nozzle throat section:

$$\Theta^* = \Theta \cdot f(Ma) \tag{13}$$

III. Experimental Setup

Experimental investigations described in the present study have been performed at the European Research and Technology Test Facility P8 [29] at DLR Lampoldshausen using subscale combustion chamber E [23].

A. Subscale Combustion Chamber E

Subscale combustion chamber E (see Fig. 2) can guarantee stable operation for a combustion-chamber pressure up to $p_{cc} = 15$ MPa in combination with a nearly stoichiometric mixture ratio ROF. This subscale combustion chamber covers the full operating range of the European Vulcain 2 engine for the Ariane 5 launcher ($p_{cc} =$ 11.5 MPa and $ROF = 7.3$) with an additional extension of this operating range. The combustion chamber features a cylindrical segment of 200 mm with a diameter of 50 mm and a nozzle segment with a nozzle throat diameter of 33 mm. The cylindrical segment and the nozzle segment are cooled by water flowing through drilled (cylindrical segment) or milled (nozzle segment) cooling channels.

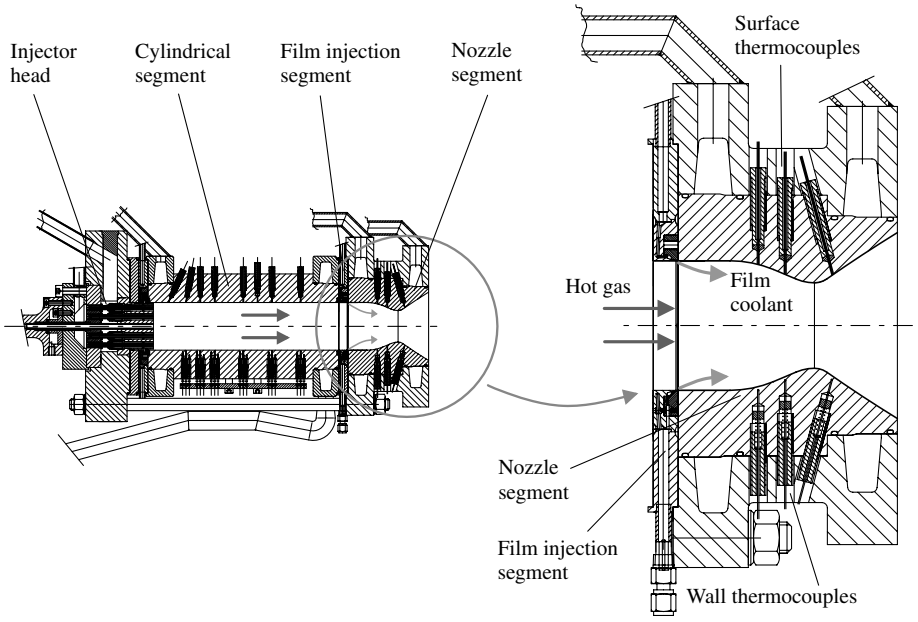

Fig. 2 Subscale combustion chamber E.

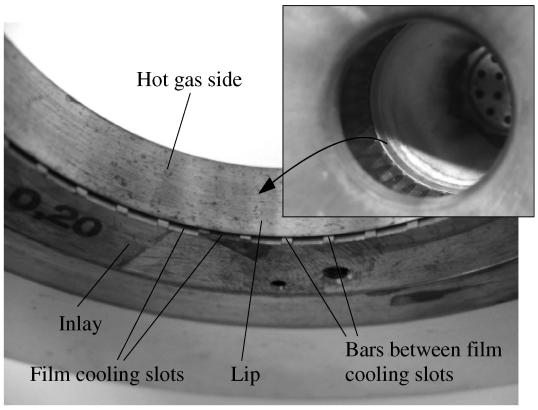

Fig. 3 Film coolant injection segment.

For detecting the film cooling effectiveness inside the rocket combustion chamber downstream of the film injection point, the nozzle segment is equipped with two rows of surface thermocouples, which allow direct measurement of the local hot-gas-side wall temperatures inside the combustion chamber, and four rows of wall thermocouples with a wall distance of $d = 1$ mm (see Fig. 2). To describe film cooling effectiveness with an accelerated hot gas, the thermocouples are arranged in the sub- and supersonic parts of the nozzle segment, with two additional wall thermocouples at the nozzle throat. As a result of vibrations up to100 g and material expansion and contraction during the hot run, a loss of mechanical contact of the wall thermocouples can occur. Thus, a spring system has been developed at DLR Lampoldshausen to provide a constant force to ensure reliable contact of all wall thermocouples during the hot-run tests [30].

B. Film Coolant Injection Segment

The film coolant injection segment has been arranged between the cylindrical and the nozzle segments of the subscale combustion chamber (see Fig. 2). To provide a uniform film coolant distribution in the circumferential direction, an almost continuous film injection slot has been used. Bars for bracing the thin lip of the injection segment against the impact of thermal and structural loads guarantees a constant film slot height during a hot run (see Fig. 3). Because of the thin lip with a lip thickness $t \approx 0$ at the point of injection, an almost continuous contour with minimal disturbance of the hot gas is achieved.

Figure 4a shows the buildup of the film coolant injection segment. The main structure contains 50 bore holes for uniform coolant

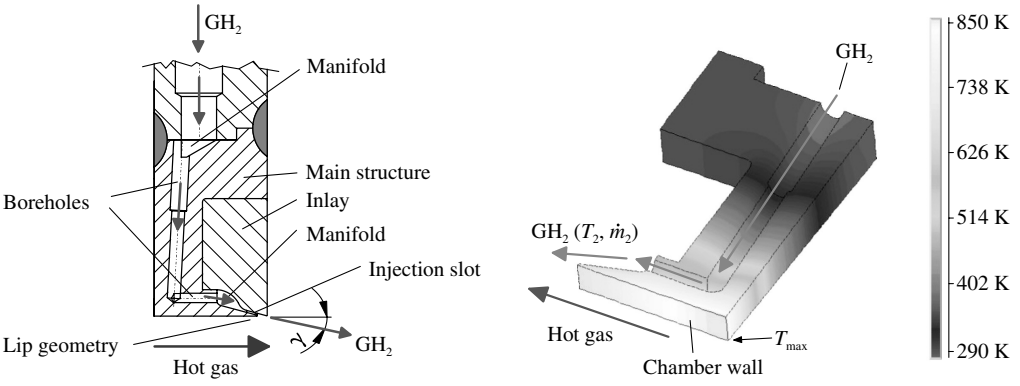

a) Buildup of the film coolant injection segment

b) Temperature distribution in the film coolant injection segment

Fig. 4 Film coolant injection segment.

Table 1 Data of the film coolant injection segment

Number of slots	40
Slot height s, mm	0.2 ± 0.015
Slot width b, mm	3.0 ± 0.015
Injection angle γ, deg	15

distribution and the inlay provides the film coolant slots and bars. The coolant is injected almost tangentially with an angle of $\gamma = 15$ deg between the hot gas and coolant into the hot-gas stream. Because the film coolant not only has the task of protecting the chamber wall from hot-gas impact downstream of the point of injection, but also cools the structure of the film injection segment itself before entering the combustion chamber, numerical modeling was used to optimize the coolant flow inside the injection segment and the temperature distribution of the structure. Figure 4b displays the calculated temperature distribution of the film coolant injection segment for a test case with $p_{cc} = 13$ MPa and $ROF = 7.3$, using 0.1 kg/s hydrogen at a temperature of 290 K as a film coolant. Because the maximum wall temperature occurs in the hot-gas-side corner opposite to the film injection, biasing of the GH_2 supply bore holes reduces the heat load at this position.

Because precise knowledge of the injected film temperature T_2 is essential for describing the effectiveness of the film downstream of the point of injection, two thermocouples were attached to measure the coolant temperature inside the manifold just before the hydrogen entered the combustion chamber.

Table 1 gives an overview of the dimensions of the film injection-segment geometry. The axial distance between film coolant injection and the nozzle throat of the combustion chamber is 52.5 mm. For future research investigations, it is possible to change the slot geometry and slot number of the inlay because of the modular design of the film coolant injection segment.

C. Operating Conditions

Tests at three pressure levels have been performed: 12 MPa (Vulcain-2-like conditions), 8 MPa (advanced upper-stage engine conditions), and 5 MPa (upper-stage engine conditions) with a constant mixture ratio $ROF = 6$ (see Fig. 5a). Each pressure step has been divided into three sections with differing coolant mass flow rates $\dot{m}_2$, which gave nine different operating conditions for each hot run (see Fig. 5b). A reference case with no film cooling was performed by removing the film coolant injection segment between cylindrical and nozzle segment.

Table 2 gives an overview of the hot-gas conditions such as combustion-chamber pressure p_{cc}, injector-head mass flow rate $\dot{m}_{tot}$, and propellant injection temperatures T_{H_2} and T_{O_2}.

Table 3 features a summary of the film cooling parameters such as film blowing rate M, film injection temperature T_2, and velocity ratio between hot gas and film coolant u_2/u_{cc}. Hydrogen has been used for all tests as a film coolant.

IV. Experimental Results

Figure 6 shows the TDK91/PRO [10] calculated trends of temperature ratio T/T_{max}, pressure ratio p/p_{max}, and local Mach number Ma as a function of the nozzle-segment contour D/D_t of subscale combustion chamber E (see Fig. 2) for a combustion-chamber pressure $p_{cc} = 12$ MPa and a film blowing rate $M = 0$.

For film cooling investigations in the nozzle segment, the film coolant is injected at the axial position $x/s = 0$, and acceleration of the flow starts about 100 slot heights downstream of the film coolant injection (see Fig. 6). Very strong acceleration effects cause an increase of the hot-gas flow velocity by a factor ≈ 8 in the axial direction in only a few centimeters.

Heat flux densities up to almost 100 MW/m^2 in the nozzle throat region of the subscale combustion chamber result in thermal gradients of more than 300 K/mm inside the copper liner in close proximity to the hot-gas side. Even very small radial errors in thermocouple installation may result in significant deviations of the experimental data. So although there are numerical methods such as the inverse heat transfer problem that could be used in theory, very high heat flux densities prevent a convergence of the equations and therefore a solution of the problem. On this account, inverse heat transfer will not be considered in the following analysis.

Although both wall thermocouples and surface thermocouples have been used in the nozzle segment (see Fig. 2) to describe the film cooling influence, very high heat fluxes and temperatures in the nozzle throat section have resulted in a high failure rate of the surface thermocouples. For this reason, the following description of film cooling effectiveness with accelerated hot gas is predominantly based on the results of the wall thermocouples, located at a constant wall distance $d = 1$ mm inside the copper liner.

Because of the application of the wall thermocouples with a constant wall distance d in the nozzle segment, film cooling effectiveness following Eq. (3) cannot be used here. As a result of the axial variation of thermal heat fluxes and wall temperatures in the nozzle segment, the film injection temperature T_2 can be higher than the temperature inside the chamber wall (see Fig. 7). As the case may be, film cooling effectiveness calculated with the use of Eq. (3) would indicate a misleadingly high or even negative film cooling effectiveness in the area of accelerated hot gas.

On this account, film cooling effectiveness with accelerated hot gas Θ^*, measured by wall thermocouples (wall distance $d > 0$) in the nozzle segment, will only be related to the local wall temperature without film cooling:

$$\Theta^*_{d>0} = \frac{T_{W,0} - T_{W,f}}{T_{W,0}} \tag{14}$$

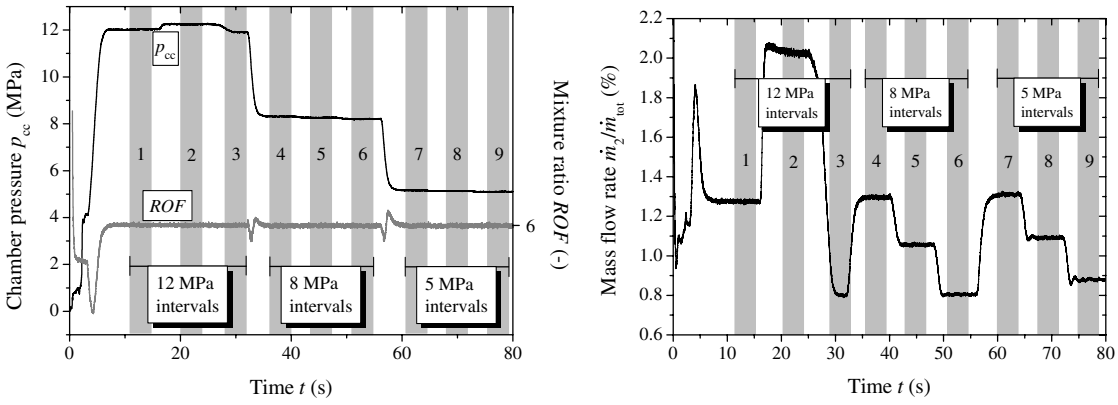

a) Combustion chamber pressure and mixture ratio **b) Film coolant mass flow rate**

Fig. 5 Operating conditions.

Table 2 Hot-gas conditions

Interval	1	2	3	4	5	6	7	8	9
p_{cc}, MPa	12.0	12.2	11.9	8.3	8.3	8.2	5.2	5.1	5.1
ROF	6.0	6.0	6.0	6.0	6.0	6.0	6.0	6.0	6.0
$\dot{m}_{tot}$, kg/s	4.22	4.22	4.21	2.93	2.93	2.93	1.84	1.84	1.84
T_{H_2}, K	287.9	285.5	283.1	278.8	278.4	277.3	277.1	276.2	274.9
T_{O_2}, K	113.5	111.5	111.2	112.8	113.3	113.2	114.8	115.2	115.6

Table 3 Film cooling parameters

Interval	1	2	3	4	5	6	7	8	9
$\dot{m}_2/\dot{m}_{tot}$, %	1.28	2.04	0.83	1.30	1.06	0.82	1.31	1.09	0.87
T_2, K	321.3	307.0	335.3	323.9	331.1	340.7	324.8	330.7	338.1
M	1.08	1.73	0.72	1.09	0.90	0.71	1.10	0.93	0.76
u_2/u_{cc}	0.67	1.00	0.46	0.68	0.57	0.45	0.68	0.58	0.48

To estimate deviations between $\Theta^*_{d>0}$ in Eq. (14) and the film cooling effectiveness Θ (respectively, Θ^* for accelerated flow), defined in Eq. (3), the difference in film cooling effectiveness comparing Θ^* and $\Theta^*_{d>0}$ can be written as

$$\Delta\Theta^* = \frac{\Theta^* - \Theta^*_{d>0}}{\Theta^*} \tag{15}$$

With the use of experimental film cooling data obtained during a different test campaign at DLR Lampoldshausen ($p_{cc} = 11.5$, 8, and 5 MPa at $ROF = 6$) investigating tangential slot injection with gaseous hydrogen as a film coolant in close proximity of the coaxial injector head [23,24,31] in the cylindrical segment of subscale combustion chamber E, a relatively simple correction factor $f(\Delta\Theta^*)$ was found to compensate for deviations of Θ^* and $\Theta^*_{d>0}$, where parameters a_1 and a_2 depend on the film blowing rate M:

$$f(\Delta\Theta^*) = 1 - \left(a_1 + \frac{a_2}{(x/s)^{0.5}}\right) \tag{16}$$

Equation (16) only depends on measurement application in the liner wall material. Figure 8 shows the difference in film cooling effectiveness $\Delta\Theta^*$ for a combustion-chamber pressure of 11.5 MPa at two different blowing rates M in the cylindrical segment of subscale combustion chamber E. Deviations of $\Theta^*_{d>0}$ compared with the film cooling effectiveness Θ^* are about 40% in close proximity of the film injection point ($x/s \approx 100$), with a fast decrease and a gradual approach to $\Theta^*_{d>0}$ [Eq. (14)] and Θ [Eq. (3)] farther downstream.

To a first approximation, deviation $\Delta\Theta^*$ is a function of film cooling length x/s and film blowing rate M, whereas the influence of the combustion-chamber pressure p_{cc} can be neglected for the investigated pressure intervals.

Finally, because correction factor $f(\Delta\Theta^*)$ is dependent on the wall distance d of the measured temperatures, as mentioned previously, it can be written in general:

$$f(\Delta\Theta^*) = \begin{cases} f(x/s), M);\ \text{Eq.(16)} & \text{for } d > 0 \\ 1 & \text{for } d = 0 \end{cases} \tag{17}$$

To evaluate the influence of hot-gas acceleration on the film cooling effectiveness, comparison of experimental data with the modified film cooling model from Goldstein and Haji-Sheikh [13], developed for film cooling effectiveness in the cylindrical part of the

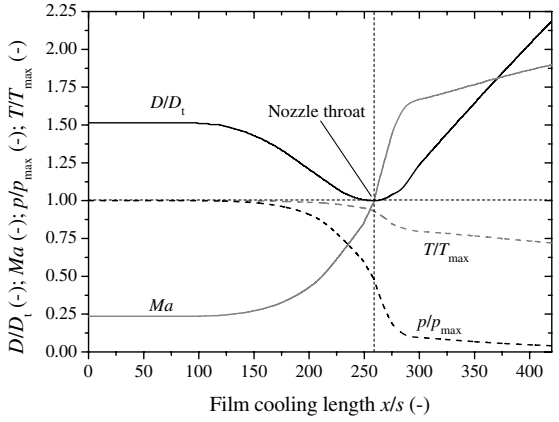

Fig. 6 Parameters for accelerated flow ($p_{cc} = 12$ MPa).

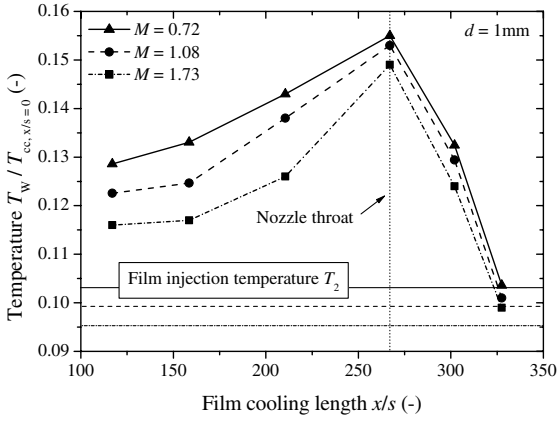

Fig. 7 Wall temperature distribution in the nozzle segment ($p_{cc} = 12$ MPa).

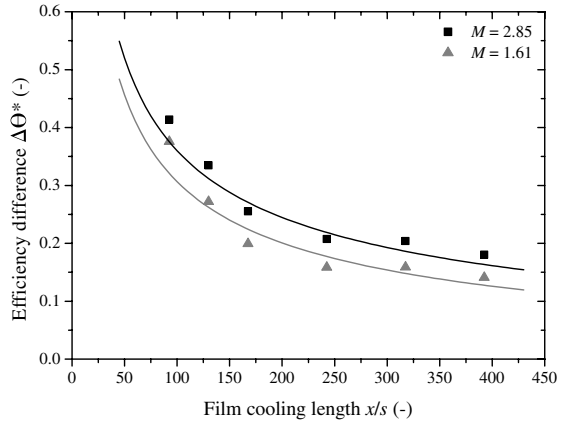

Fig. 8 Film cooling effectiveness difference $\Delta\Theta^*$ ($p_{cc} = 11.5$ MPa).

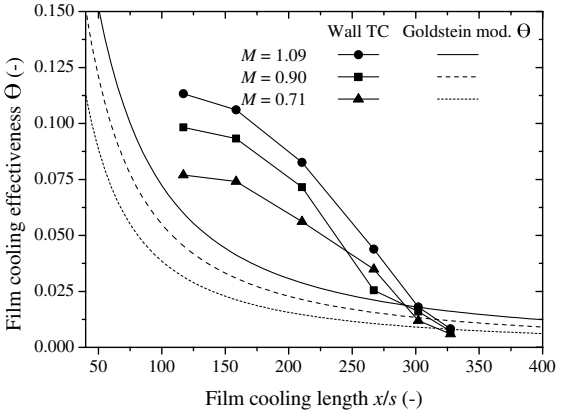

Fig. 9 Comparison of film cooling model for nonaccelerated flow with measured data ($p_{cc} = 8$ MPa).

subscale combustion chamber [24] [Eq. (11)], has been done (see Fig. 9). However, compared with the relatively good agreement between experimental data from the wall thermocouples (wall TC) and the modified Goldstein and Haji-Sheikh [13] model following Eq. (11) [24], a somewhat higher deviation can be found downstream of the film injection point ($x/s \approx 100, \ldots, 250$). The measured film cooling effectiveness in the nozzle segment seems to be higher in close proximity of the film injection point than predicted by the modified Goldstein and Haji-Sheikh [13] model for nonaccelerated flow.

Whereas most film cooling models [13,15,17,18,32] scale the effectiveness as a function of nondimensional distance $(x/s)^{-0.8}$, experimental film cooling investigations in the cylindrical segment [24] and in the nozzle segment at DLR Lampoldshausen gave much better characterization using the effectiveness in terms of distance $\approx (x/s)^{-1.4}$.

Further-developed flow characteristics in the nozzle segment in comparison with the nondeveloped starting flow in close proximity to the injector head, in which atomization and combustion processes are dominant, may result in a higher film cooling effectiveness. In addition, the beginning of hot-gas acceleration in the nozzle segment can improve the film cooling effectiveness compared with uniform mainstream flow [28].

Acceleration effects on film cooling effectiveness can be described by a correction factor $f(Ma)$ using the Mach number ratio between local hot-gas Mach number Ma (see Fig. 6) and the hot-gas Mach number at the point of film coolant injection, $Ma_{x/s=0}$:

$$f(Ma) = \left(\frac{Ma_{x/s=0} + Ma}{Ma} \right)^{1.5} \tag{18}$$

The empirical correction factor $f(Ma)$ is based on the experimental setup and therefore must account for the higher film cooling effectiveness at the beginning of the nozzle segment compared with data for near-injector flow with constant mainstream velocity [24]; in doing so, $f(Ma) > 1$ for the case of nonaccelerated flow ($x/s \approx 0, \ldots, 100$).

Taking into account the correction factors $f(\Delta\Theta^*)$ [Eq. (16)] and $f(Ma)$ [Eq. (18)], film cooling effectiveness for accelerated hot gas Θ^* in the nozzle segment of the subscale rocket combustion chamber in consideration of Eqs. (11) and (13) is finally given by

$$\Theta^* = \frac{0.83 Pr^{2/3}}{1.11 + 0.329(c_{p,cc}/c_{p,2})[(x/s)(1/M)]^{1.43} Re_{2,s}^{-0.25}} \cdot f(\Delta\Theta^*) \cdot f(Ma) \tag{19}$$

As shown in Fig. 10, a good agreement between film cooling effectiveness using Eq. (19) and measured experimental data is achieved for the investigated pressure intervals 12, 8, and 5 MPa at various film blowing rates M. Although a much steeper gradient is predicted by the film cooling model in the proximity of the film coolant injection point ($x/s \approx 100, \ldots, 200$), the decrease in the film

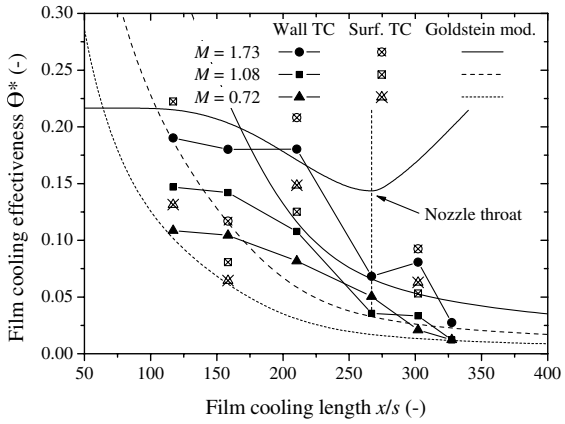

a) $p_{cc} = 12$ MPa

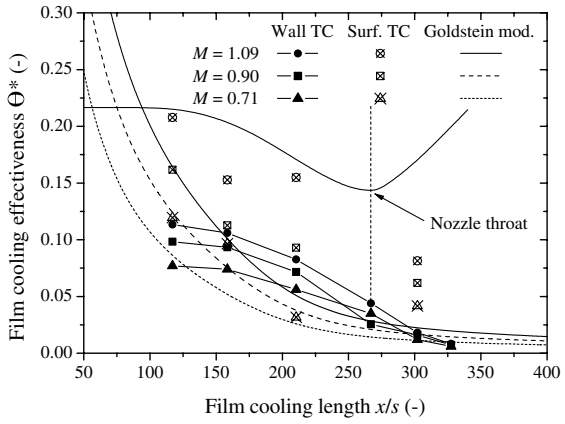

b) $p_{cc} = 8$ MPa

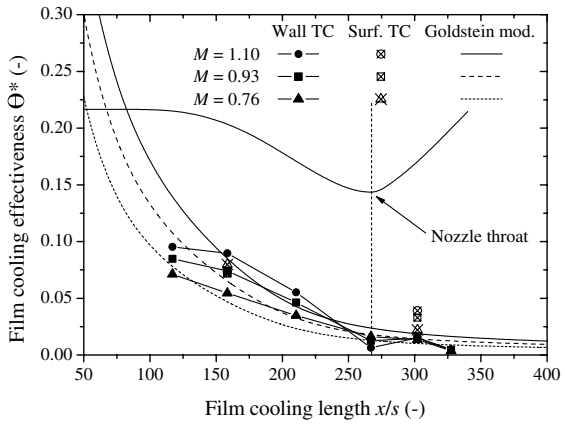

c) $p_{cc} = 5$ MPa

Fig. 10 Film cooling effectiveness.

cooling effectiveness with axial distance is specified persuasively by Eq. (19).

Comparable with film cooling investigations in the cylindrical segment [23,24,33], the influence of the combustion-chamber pressure p_{cc} on film cooling effectiveness with accelerated hot gas is also small by way of comparison ($M = 0.72$, 0.71, and 0.76 at $p_{cc} = 12$, 8, and 5 MPa, respectively). The film blowing rate M can be identified as a main parameter on film cooling effectiveness. An increase of the film blowing rate indicates a significant rise of film cooling effectiveness, not only close to the film injection point, but also farther downstream. The correlation between the film blowing rate and local film effectiveness is almost linear, as a comparison of $M = 1.73$ and 1.08 at $p_{cc} = 12$ MPa displays.

Results measured by surface thermocouples and wall thermocouples show a good match at certain axial distances. Because of the arrangement in the nozzle segment, surface and wall thermocouples

Table 4 Reproducibility of hot-gas conditions

Interval	1	2	3	4	5	6	7	8	9
$p_{cc,A}/p_{cc,B}$	0.996	0.997	0.996	0.997	0.997	0.996	0.997	0.996	0.997
ROF_A/ROF_B	0.998	0.997	0.998	0.998	0.998	0.998	0.997	0.998	0.997

Table 5 Reproducibility of measured temperatures

x/s	117	158.5	210.5	267	302	327.5
$T_{W,A}/T_{W,B}$, wall thermocouples	0.995	0.987	1.006	1.003	0.989	0.991
$T_{W,A}/T_{W,B}$, surface thermocouples	0.974	0.973	1.018	——	0.977	——

are located at different angular positions. High turbulence levels of the hot-gas flow can also induce variations of heat flux and temperature in the circumferential direction and thereby give different film-cooling-effectiveness values.

V. Error Analysis

The absolute accuracy of the measured data is just as important as the reproducibility of the experiment. The heat load inside a rocket combustion chamber is predominantly driven by the combustion-chamber pressure p_{cc} [see Eq. (1)] and the propellant mixture ratio ROF. The comparison of two hot runs A and B with identical P8 test bench conditions (see Table 4) shows the excellent reproducibility of the test bench and therefore the reproducibility of the hot-gas condition inside the combustion chamber.

Comparable good results have been achieved with the measured temperatures (see Table 5 for maximum deviation at various axial positions x/s). The deviation of the results of the wall thermocouples is up to 2%, whereas a slightly higher deviation up to 3% has been measured when using the surface thermocouples. Assuming a hot-gas-side wall temperature of 800 K, the maximum fluctuation range between two hot runs can be estimated with ≈14 and 20 K if worse comes to worst, using wall thermocouples and surface thermocouples, respectively.

Taking into account measurement errors due to the application in the chamber wall, the following estimation can be done to judge the film-cooling-effectiveness errors: 1) $\Delta\Theta^* \approx 0.002, \ldots, 0.03$ when using wall thermocouples and 2) $\Delta\Theta^* \approx 0.003, \ldots, 0.06$ when using surface thermocouples.

In consideration of the large-scale tests with a Vulcain 2, such as a hot-gas situation, the errors in describing temperatures and film cooling results in the subscale rocket combustion chamber are good by way of comparison.

VI. Conclusions

In the present study, film cooling effectiveness in a nozzle segment of a subscale rocket combustion chamber has been investigated. Using wall thermocouples as well as surface thermocouples, a detailed temperature distribution in sub-, trans-, and supersonic conditions has been used to describe film cooling effectiveness with accelerated hot gas. Gaseous hydrogen has been injected with an angle of $\gamma = 15$ deg between coolant flow and hot gas through 40 film cooling slots distributed evenly in the circumferential direction, with the coolant injection segment arranged just before the converging part of the nozzle segment. Three major pressure intervals ($p_{cc} = 12, 8$, and 5 MPa) with various film blowing rates M were carried out, simulating representative thermal conditions with heat fluxes in the nozzle throat section of more than 100 MW/m^2.

Because of a more fully developed flow compared with the flow in close proximity to the injector head in the cylindrical part of the subscale combustion chamber, higher film effectiveness has been detected at the beginning of the nozzle segment for comparable hot-gas and film coolant conditions.

Because there are no existing film cooling models describing film cooling effectiveness with accelerated hot gas in a rocket combustion chamber, a modified film cooling model has been used to implement an additional correction factor regarding the local Mach number Ma for film cooling effectiveness in accelerated flow. Film blowing rate M has been detected as a main parameter for film cooling effectiveness with accelerated hot gas, whereas the influence of the combustion-chamber pressure is significantly smaller. Convincing agreement between modified film cooling prediction and experimental data of both wall thermocouples and surface thermocouples over a wide range of combustion-chamber pressure and film blowing rates $M < 1$ as well as $M > 1$ shows the applicability of this film cooling model in combination with accelerated hot gas.

Further experimental investigations at DLR Lampoldshausen will take into account the influence of slot height and velocity ratio of film coolant and hot gas on film cooling effectiveness with accelerated hot gas.

Acknowledgment

The authors would like to acknowledge the P8 team for their assistance at the test campaign.

References

[1] Bartz, D. R., "A Simple Equation for Rapid Estimation of Rocket Nozzle Convective Heat Transfer Coefficients," *Journal of Jet Propulsion*, Jan. 1957, pp. 49–51.

[2] Sutton, G. P., "History of Liquid-Propellant Rocket Engines in Russia, Formerly the Soviet Union," *Journal of Propulsion and Power*, Vol. 19, No. 6, 2003, pp. 1008–1037. doi:10.2514/2.6943

[3] Sutton, G. P., "History of Liquid Propellant Rocket Engines in the United States," *Journal of Propulsion and Power*, Vol. 19, No. 6, 2003, pp. 978–1007. doi:10.2514/2.6942

[4] Huzel, D. K., and Huang, D. H., *Modern Engineering for Design of Liquid-Propellant Rocket Engines*, Progress in Astronautics and Aeronautics, Vol. 147, AIAA, Washington, D.C., 1992.

[5] Sutton, G. P., Wagner, W. R., and Seader, J. D., "Advanced Cooling Techniques for Rocket Engines," *Astronautics and Aeronautics*, Vol. 1, Jan. 1966, pp. 60–71.

[6] Strakey, P. A., Talley, D. G., Tseng, L. K., and Miner, K. I., "Effects of Liquid-Oxygen Post Biasing on SSME Injector Wall Compatibility," *Journal of Propulsion and Power*, Vol. 18, No. 2, Mar.–Apr. 2002, pp. 240–246. doi:10.2514/2.5954

[7] Fröhlich, A., Popp, M., and Thelemann, D., "Heat Transfer Characteristics of H2/O2—Combustion Chambers," 29th AIAA/SAE/ASME/ASEE Joint Propulsion Conference, Monterey, CA, AIAA Paper 93-1826, June 1993.

[8] Terry, J. E., and Caras, G., "Transpiration and Film Cooling of Liquid Rocket Nozzles," U.S. Army Missile Command, Redstone Scientific Information Center, Rept. N 66 38728, Redstone Arsenal, AL, Mar. 1966.

[9] Volkmann, J. C., McLeod, J. M., and Claflin, S. E., "Investigation of Throat Film Coolant for Advanced LOX/RP-1 Thrust Chambers," 27th AIAA/SAE/ASME/ASEE Joint Propulsion Conference, Sacramento, CA, June 1991, AIAA Paper 91-1979.

[10] Dunn, S. S., Coats, D. E., Nickerson, G. R., and Berker, D. R., *Two-Dimensional Kinetics (TDK91/PRO) Nozzle Performance Computer Program*, Software and Engineering Associates, Inc., Carson City, NV, Nov. 1991.

[11] Ziebland, H., and Parkinson, R. C., "Heat Transfer in Rocket Engines," AGARD AGARDograph AG-148-71, Neuilly-sur-Seine, France, 1971.
[12] Goldstein, R. J., "Film Cooling," *Advances in Heat Transfer*, Vol. 7, 1971, pp. 321–379.
[13] Goldstein, R. J., and Haji-Sheikh, A., "Prediction of Film Cooling Effectiveness," Japan Society of Mechanical Engineers Paper 225, Sept. 1967.
[14] Eckert, E. R. G., and Birkebak, R. C., "The Effects of Slot Geometry on Film Cooling," *Heat Transfer, Thermodynamics, and Education*, edited by H. A. Johnson, McGraw–Hill, New York,1964, pp. 150–163.
[15] Stollery, J. L., and El-Ehwany, A. A. M., "A Note on the Use of a Boundary Layer Model for Correlating Film Cooling Data," *International Journal of Heat and Mass Transfer*, Vol. 8, 1965, pp. 55–65.
doi:10.1016/0017-9310(65)90097-9
[16] Tribus, M., and Klein, J., "Forced Convection from Nonisothermal Surfaces," *Proceedings of the Heat Transfer Symposium*, Univ. of Michigan Press, Ann Arbor, MI, 1953, pp. 211–235.
[17] Kutateladze, S. S., and Leont'ev, A. I., "The Heat Curtain in the Turbulent Boundary Layer of a Gas," *Thermal Physics of High Temperature*, Vol. 1, No. 2, Sept.–Oct. 1963, pp. 281–290.
[18] Librizzi, J., and Cresci, R., "Transpiration Cooling of a Turbulent Boundary Layer in an Axisymmetric Nozzle," *AIAA Journal*, Vol. 2, No. 4, Apr. 1964, pp. 617–624.
doi:10.2514/3.2397
[19] Wieghardt, K., "Über das Ausblasen von Warmluft für Enteiser," Zentrale für Wissenschaftliches Berichtswesen, Rept. FB Nr 1900, Göttingen, Germany, May 1943; also "On the Blowing of Warm Air for De-Icing Devices," Kaiser Wilhelm Inst. for Fluid Dynamics Research (in English).
[20] Goldstein, R. J., Shavit, G., and Chen, T. S., "Film Cooling Effectiveness with Injection Through a Porous Section," *Journal of Heat Transfer*, Vol. 87, Aug. 1965, pp. 353–361.
[21] Goldstein, R. J., Rask, R. B., and Eckert, E. R. G., "Film Cooling with Helium Injection into an Incompressible Air Flow," *International Journal of Heat and Mass Transfer*, Vol. 9, 1966, pp. 1341–1350.
doi:10.1016/0017-9310(66)90132-3
[22] Nishiwaki, N., Hirata, M., and Tsuchida, A., "Heat Transfer on a Surface Covered by a Cold Air Film," *International Developments in Heat Transfer*, Pt. 4, American Society of Mechanical Engineers, New York, 1961, pp. 675–681.
[23] Arnold, R., Suslov, D., Weigand, B., and Haidn, O. J., "Investigation of Film Cooling in a High Pressure LOX/GH_2 Subscale Combustion Chamber," Space Propulsion 2008, Crete, Greece, ESA Paper 42-090, May 2008.
[24] Arnold, R., Suslov, D., Weigand, B., and Haidn, O. J., "On Film Cooling in a High Pressure LOX/GH_2 Subscale Combustion Chamber: Tangential Slot Injection," *Aerospace Science and Technology* (submitted for publication).
[25] Seban, R. A., and Back, L. H., "Effectiveness and Heat Transfer for a Turbulent Boundary Layer with Tangential Injection and Variable Freestream Velocity," *Journal of Heat Transfer*, Vol. 84, 1962, pp. 235–244.
[26] Hartnett, J. P., Birkebak, R. C., and Eckert, E. R. G., *Velocity Distribution, Temperature Distributions, Effectiveness and Heat Transfer in Cooling of a Surface with a Pressure Gradient*, Vol. 4, American Society of Mechanical Engineers, New York, 1961, pp. 682–689.
[27] Escudier, M. P., and Whitelaw, J. H., "The Influence of Strong Adverse Pressure Gradients on the Effectiveness of Film Cooling," *International Journal of Heat and Mass Transfer*, Vol. 11, 1968, pp. 1289–1292.
doi:10.1016/0017-9310(68)90198-1
[28] Carlson, L. W., and Talmor, E., "Gaseous Film Cooling at Various Degrees of Hot-Gas Acceleration and Turbulence Levels," *International Journal of Heat and Mass Transfer*, Vol. 11, 1968, pp. 1695–1713.
doi:10.1016/0017-9310(68)90048-3
[29] Fröhlke, K., Haberzettel, A., Haidn, O. J., Heinrich, S., Sion, M., and Vuillermoz, P., "First Hot Fire Test Campaign at the French-German Research Facility P8," 33rd AIAA/ASME/SAE/ASEE Joint Propulsion Conference and Exhibit, Seattle, WA, AIAA Paper 97-2929, July 1997.
[30] Suslov, D., Woschnak, A., Sender, J., and Oschwald, M., "Test Specimen Design and Measurement Technique for Investigation of Heat Transfer Processes in Cooling Channels of Rocket Engines Under Real Thermal Conditions," 24th International Symposium on Space Technology and Science, Miyazaki, Japan, ISTS Paper 2004-e-40, 2004.
[31] Arnold, R., Suslov, D., Weigand, B., and Haidn, O. J., "Circumferential Behavior of Tangential Film Cooling and Injector Wall Compatibility in a High Pressure LOX/GH_2 Subscale Combustion Chamber," 44th AIAA/ASME/SAE/ASEE Joint Propulsion Conference and Exhibit, Hartfort, CT, AIAA Paper 2008-5242, July 2008.
[32] Hartnett, J. P., Birkebak, R. C., and Eckert, E. R. G., "Velocity Distributions, Temperature Distributions, Effectiveness and Heat Transfer for Air Injected Through a Tangential Slot into a Turbulent Boundary Layer," *Journal of Heat Transfer*, Vol. 83, Aug. 1961, pp. 293–306.
[33] Arnold, R., Suslov, D., and Haidn, O. J., "Experimental Investigation of Film Cooling with Tangential Slot Injection in a LOX/CH_4 Subscale Rocket Combustion Chamber," 26th International Symposium on Space Technology and Science, Hamamatsu, Japan, Paper 2008-a-05, June 2008.

D. Talley
Associate Editor